Modelling of nitrogen implantation processes into WC-Co indexable knives for wood-based material machining using ion implanters with or without direct ion beam

MAREK BARLAK[1], JACEK WILKOWSKI[2], ZBIGNIEW WERNER[1]
[1] Plasma/Ion Beam Technology Division (FM2), National Centre for Nuclear Research Świerk - NCBJ
[2] Department of Mechanical Processing of Wood, Warsaw University of Life Sciences - SGGW

Abstract: *Modelling of nitrogen implantation processes into WC-Co indexable knives for wood-based material machining using ion implanters with or without direct ion beam.* The paper presents the results of modelling of the depth profiles of nitrogen implanted to W-C-Co material using ion implanters with or without direct ion beam. The modelling was performed using the Monte Carlo method. The results were obtained for one fluence of the implanted ions and three different values of the acceleration voltage.

Keywords: WC-Co composites, ion implantation, modelling, Monte Carlo method

INTRODUCTION

Cemented tungsten carbides - a combination of hard and brittle carbides and a relatively soft and ductile metallic binder, gives rise to an exceptional combination of attractive properties such as strength, hardness, fracture toughness, refractoriness, stiffness, resistance to compressive deformation and wear resistance at room as well as at higher temperatures up to 400°C (Milman et al. 1997, Sheikh-Ahmad and Bailey 1999, Pirso et al. 2004, Bonny et al. 2010, Choi et al. 2010, Olovsjö et al. 2013). Unfortunately, the durability of tools made of this material is still insufficient. There are several methods to improve this property, ion implantation being one of them (Barlak et al. 2016, Barlak et al. 2017). This low temperature method is used in material engineering processes to modify/change the physical and/or chemical properties of the near-surface regions of solid materials (targets) through the introduction of foreign element(s) ions. The introduced ions are accelerated in the electric field to an energy from several dozen to several hundred kiloelectronvolts, which corresponds to their velocity from hundreds to thousands of kilometres per second. The ion beam interacts with the modified material, introduces new atoms, damages its crystal lattice, creates vacancies and other defects up to total amorphisation. The substrate atoms and early implanted atoms are ejected from the surface (Fig. 1). The modified region is not an additional layer, hence no adhesion problem occurs (no delamination), and the change of dimensions and of the surface finish of the implanted material is negligible.
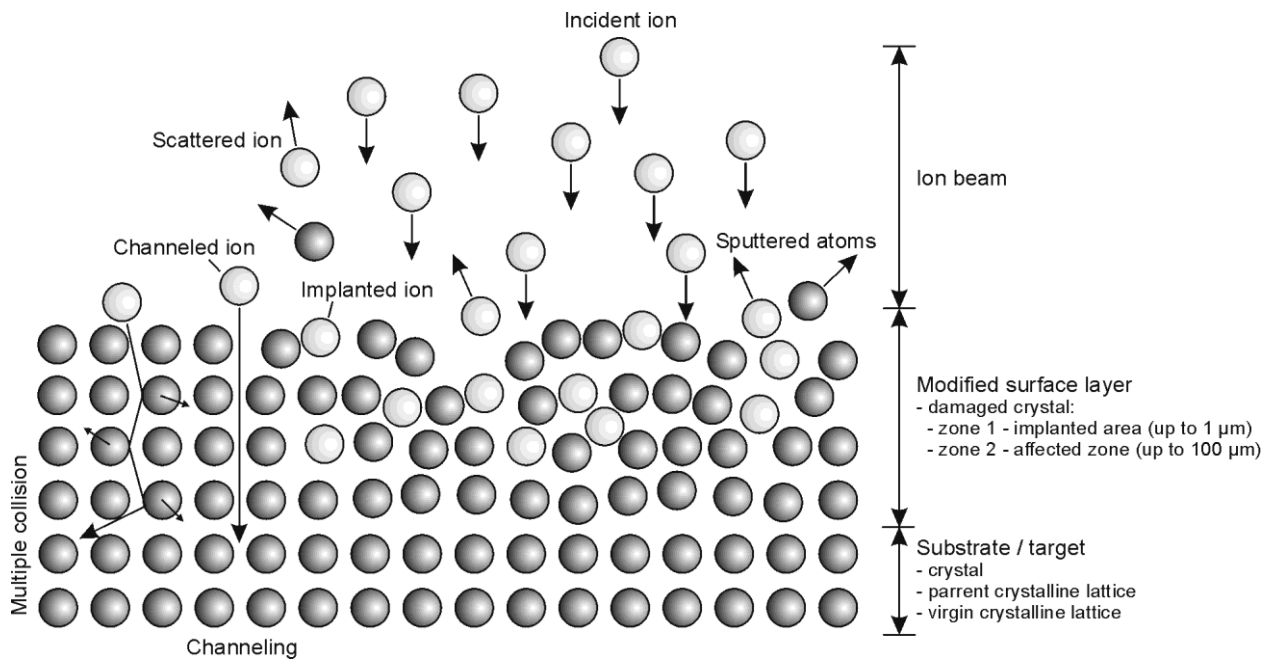
Figure 1. Diagram of the ion implantation process

There are two main types of ion implanters, i.e. implanters without mass separation (with direct ion beam) and with mass separation (without direct ion beam) - Fig. 2. A separating magnet is used for mass separation of the ion beam in order to obtain a homogenous beam in terms of constant e/m ratio.
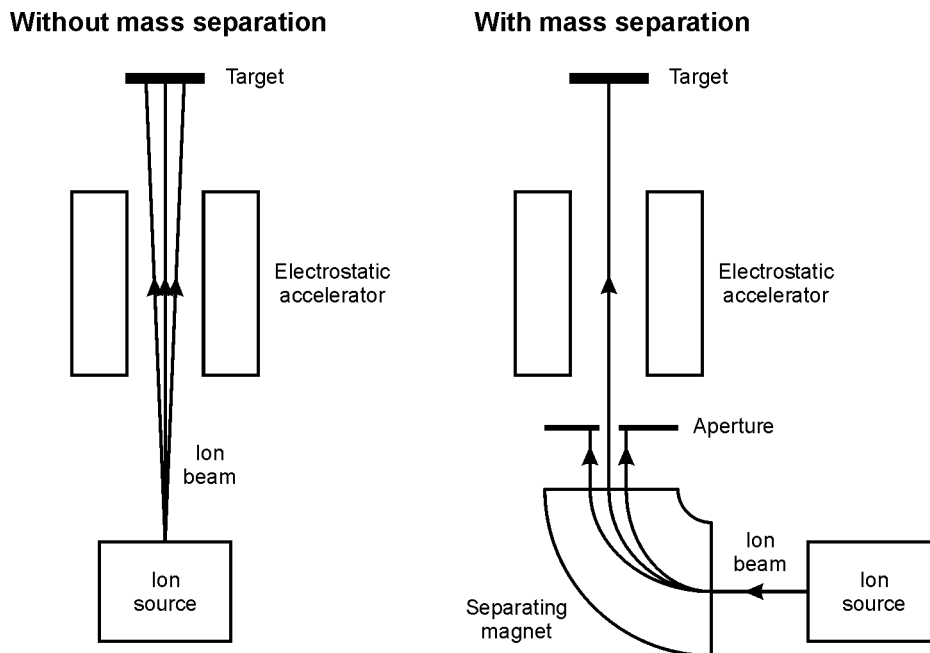

Figure 2. Diagram of an ion implanter without mass separation (left) and with mass separation (right)

The ion beam generated by an ion implanter without mass separation contains several kinds of ions with different degrees of ionization. Additionally, the percentage shares of individual ion types are also different (Table 1). The use of all data for the selected element is usually cumbersome, therefore the average charge state (ACS) is a more popular parameter for the calculation/modelling as an equivalent of the sum of profiles for the individual ion

kinds. The average charge state is determined by adding the values of multiplication of the percentage shares and the ionization's degree. For example, for yttrium it will be:

$$0.07 \cdot 1 + 0.63 \cdot 2 + 0.29 \cdot 3 + 0.01 \cdot 4 = 2.24 \approx 2.2 \qquad (1)$$

The situation is slightly different in the case of ion implantation of nitrogen. Nitrogen beam contains two kinds of ions, i.e. $N^+ + N_2^+$, in the ratio ~1:1, so there are two elementary charges per three atoms. With the acceleration voltage of 50 kV, one per three nitrogen atoms (i.e. 0.33 of atoms) carries the energy of 50 keV and two atoms (nitrogen molecule, i.e. 0.67 of atoms) carry the energy of 25 keV each. Likewise, the average charge state is at the level of 0.67.

Table 1. The percentage charge state distribution and average charge state of several elements (Krivonosienko et al. 2001 and the author's own result, unpublished)

Implanted ions	Ion energy for acceleration voltage of 50 kV (keV)						Average charge state
	25	50	100	150	200	250	
	Percentage charge state distribution (%)						
	1+		2+	3+	4+	5+	
Li^+	-	100	-	-	-	-	1.0
$N_2^+ + N^+$	67	33	-	-	-	-	0.67
$Y^+ + Y^{2+} + Y^{3+} + Y^{4+}$	-	7	63	29	1	-	2,2
$Re^+ + Re^{2+} + Re^{3+} + Re^{4+} + Re^{5+}$	-	2	26	40	26	3	3.0
$Pb^+ + Pb^{2+}$	-	40	60	-	-	-	1.6

Fig. 3 shows an example modelling of ion implantation to W-C-Co substrate material (modelling codes treat the sample as a set of atoms that do not form chemical compounds), without taking into account the phenomenon of sputtering, for two selected elements, from Table 1, i.e. for lead with two charge state ions and rhenium with five ones, for the acceleration voltage of 50 kV. The profiles named $Pb^+ + Pb^{2+}$ and $Re^+ + Re^{2+} + Re^{3+} + Re^{4+} + Re^{5+}$ were modelled for an implantation without mass separation. The ACS profiles are the equivalent of the previous profiles modelled for the average charge state. The single profiles Pb^+ and Pb^{2+} for lead and Re^+, Re^{2+}, Re^{3+}, Re^{4+} and Re^{5+} for rhenium were modelled for the individual charge state and the percentage share in the ion beam. The sum of these individual profiles should give the suitable profile $Pb^+ + Pb^{2+}$ or $Re^+ + Re^{2+} + Re^{3+} + Re^{4+} + Re^{5+}$.
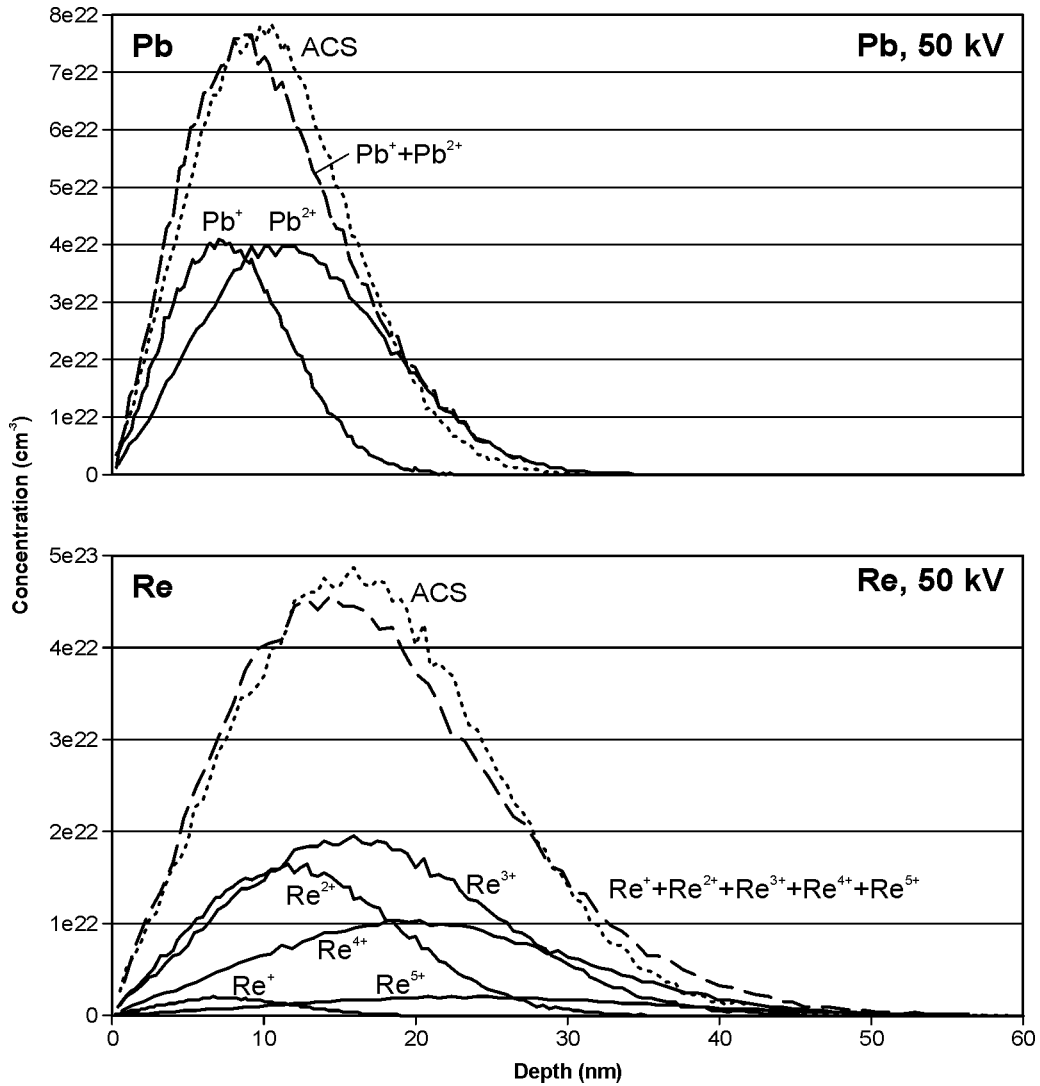
Figure 3. The modelled profiles for the ion implantation of lead and rhenium to W-C-Co substrate

All the profiles presented above have the shape close to a Gaussian curve (known also as normal distribution or bell curve) and can be defined with three main parameters, i.e. the peak volume dopant concentrations (N_{max}, cm^{-2}), the projected range (R_p, nm) and the range straggling (ΔR_p, nm) - Fig. 4 (upper, left). Sometimes, two additional parameters, i.e. the kurtosis and the skewness, are used to describe the divergence in relation to normal distribution (measures of shape).

The coefficient of kurtosis is a measure of the degree of peakedness/flatness in variable distribution - Fig. 4 (upper, right). A normal distribution is a mesokurtic distribution. A leptokurtic distribution (positive kurtosis) has a high degree of peakedness (higher peak) and heavier tails, and vice versa, a platykurtic distribution (negative kurtosis) has a low degree of peakedness (lower peak) and lighter tails.

The coefficient of skewness is a measure of the degree of asymmetry in variable distribution - Fig. 4 (lower). A positively skewed distribution, named also skewed to the right, has a tail pulled in the positive direction, and vice versa, a negatively skewed distribution, named also skewed to the left, has a tail pulled in the negative direction (Surbhi 2017).
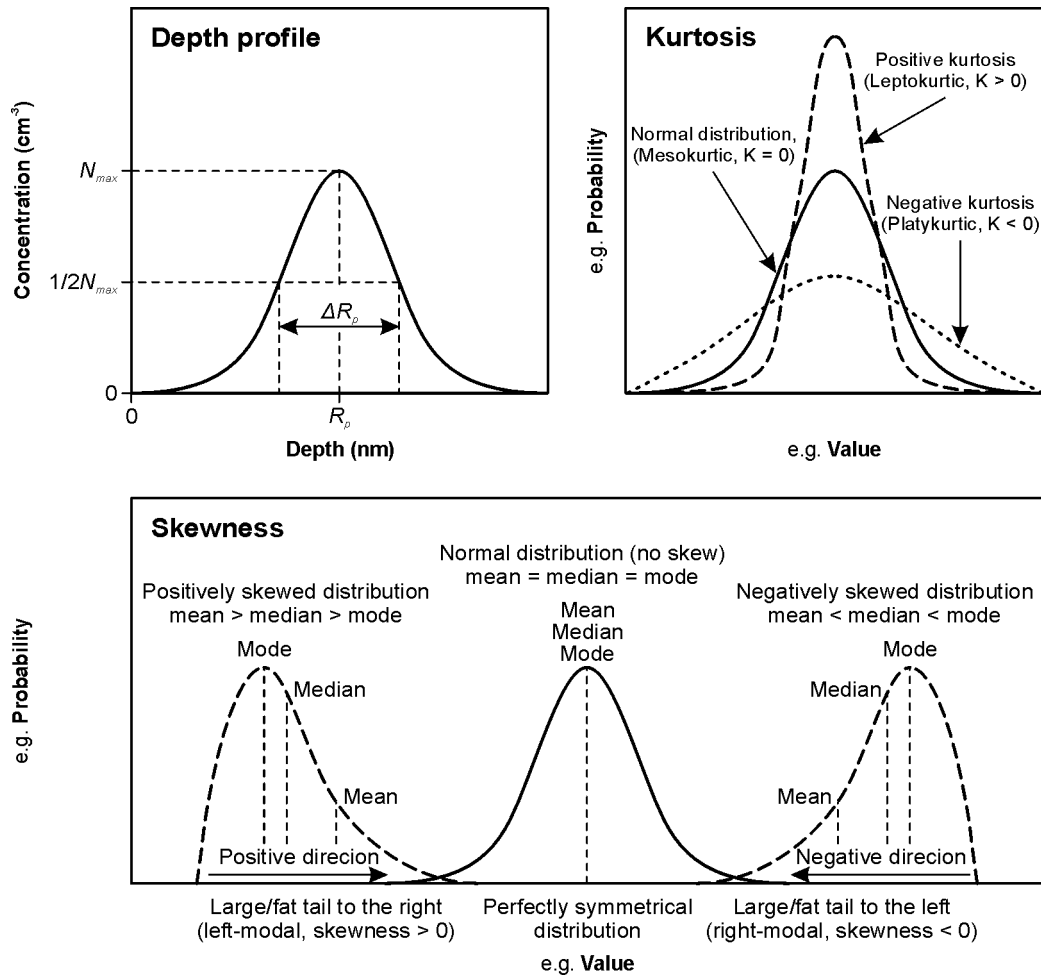
Figure 4. The graphical definitions of the main peak parameters, the kurtosis and the skewness

The present paper provides information about the modelling of nitrogen ion implantation (a typical element used to improve the durability/tribological properties) to W-C-Co material, using implanters without or with mass separation. The obtained results can be applied for example for the design of ion implantation processes of WC-Co indexable knives for wood-based material machining, as presented in Fig. 5.

This paper is an extension of the information presented in Ref. (Barlak 2019).
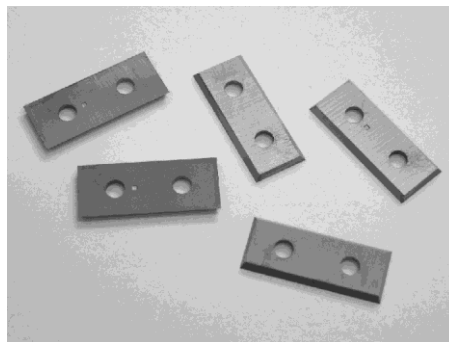

Figure 5. WC-Co indexable knives

MATERIAL AND METHODS

The $\underline{S}$topping and $\underline{R}$ange of $\underline{I}$ons in $\underline{M}$atter (SRIM-2013.00), freeware type code was used for the modelling of the depth profiles of nitrogen implanted to W-C-Co material (SRIM 2019). SRIM is a group of software packages which calculate many features of the transport of ions in matter and it includes quick calculations to generate e.g. tables of stopping powers, range and straggling distributions for any ion at any energy in any elemental target.

The SRIM code is based on a Monte Carlo simulation method. It is a method used for mathematic modelling of processes that are too complex to predict their results using an analytical approach. An important role in this method is played by draw (random selection) of quantities characterizing the process, with the random selection being carried out in accordance with a distribution that must be known (MCM 2014).

The modelling was performed for 100 000 implanted ions of nitrogen. The composition of the W-C-Co material was: 90.86% of tungsten, 5.94% of carbon and 3.2% of cobalt in weight percentages i.e. 47.4% of tungsten, 47.4% of carbon and 5.2% of cobalt in atomic percentages was defined as a target. Its density adopted for the simulation was 15.2 g/cm^3. This value was declared by the knives supplier (KCR08 type knives, by Ceratizit, Austria).

The simulations were performed for room temperature and for the total implanted fluence of 1e17 cm^{-2}, including percentage charge state distribution data from Table 1. The acceleration voltage was 5, 50 and 500 kV. The modelling did not take into account the phenomenon of substrate sputtering by the implanted ions.

The values of peak volume dopant concentrations N_{max}, projected range R_p, range straggling ΔR_p, kurtosis and skewness were determined for all nitrogen profiles, i.e. $N^+ + N_2^+$, ACS, N^+ and N_2^+, and in the next step - they were compared with the values obtained for the $N^+ + N_2^+$ profiles.

RESULTS AND DISCUSSION

Fig. 6 presents the depth profiles for all kinds of nitrogen ions i.e. $N^+ + N_2^+$, ACS, N^+ and N_2^+, for the acceleration voltage of 5, 50 and 500 kV and the fluence of 1e17 cm^{-2}. It is evident that $N^+ + N_2^+$ and ACS profiles are similar for 5 and 50 kV. A similar situation is observed when comparing the $N^+ + N_2^+$ and N_2^+ profiles, but in this case N_2^+ peak is higher and narrower than $N^+ + N_2^+$ peak, also for 5 and 50 kV. The greatest difference is observed between N^+ and $N^+ + N_2^+$ peaks. N^+ peak is lower and wider than $N^+ + N_2^+$ peak for the first two cases. The situation is different for 500 kV. In this case, the differences are large due to the saddle character of the curve of $N^+ + N_2^+$.
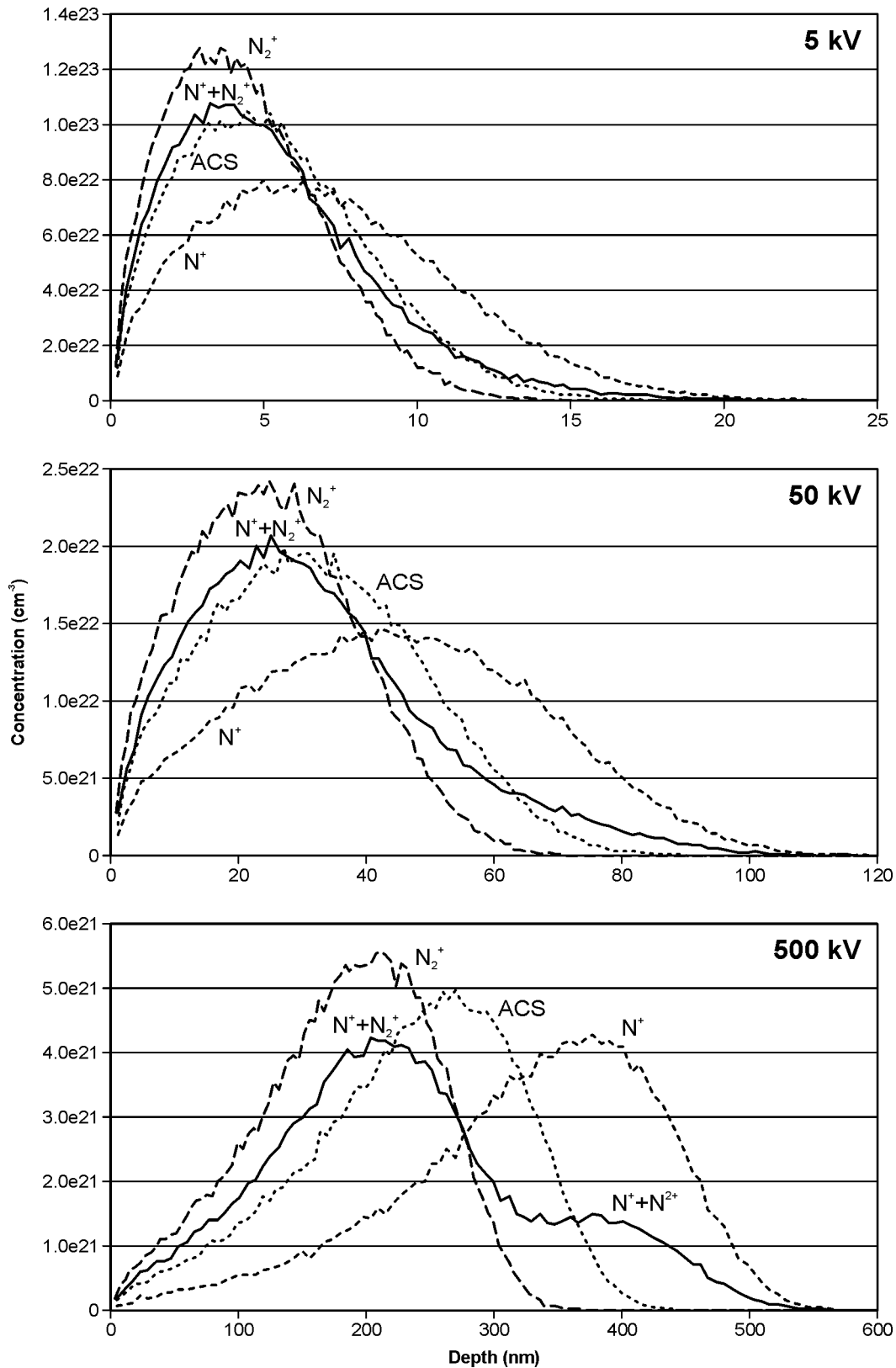
Figure 6. The depth profiles of nitrogen ions implanted to W-C-Co material

All detailed data, i.e. the values of peak volume dopant concentrations, projected range, range straggling, kurtosis and skewness, characterizing the modelled depth profiles of the implanted nitrogen, have been presented in Table 2.

Table 2. Data characterizing the modelled depth profiles of the implanted nitrogen

Implanted ions		Parameter				
		Peak volume dopant concentration N_{max} (cm^{-3})	Projected range R_p (nm)	Range straggling ΔR_p (nm)	Kurtosis	Skewness
5 kV						
without mass separated beam	$N^+ + N_2^+$	1.07e23	5.2	6.6	4.2934	1.0169
	ACS	1.05e23	5.3	6	2.8386	0.6298
with mass separated beam	N^+	7.99e22	7	7.8	2.9655	0.557
	N_2^+	1.28e23	4.3	4.8	1.1341	1.0947
50 kV						
without mass separated beam	$N^+ + N_2^+$	2.07e22	31.6	37.8	3.6237	0.8576
	ACS	1.99e22	31.8	32.4	2.4251	0.3096
with mass separated beam	N^+	1.44e22	44.4	43.8	2.4435	0.1964
	N_2^+	2.43e22	25	26	2.5837	0.3286
500 kV						
without mass separated beam	$N^+ + N_2^+$	4.22e21	230.1	210.8	1.5395	0.6113
	ACS	4.97e21	233	162.8	2.7197	-0.4509
with mass separated beam	N^+	3.98e21	325.2	200.8	1.6609	-0.4737
	N_2^+	5.56e21	181.4	136.4	2.2233	-0.2815

The percentage change of the determined values of all the above parameters in comparison to the values obtained for $N^+ + N_2^+$ profiles is presented in Table 3 and additionally, for better visualization, in Fig. 7.

The character of changes of all the parameters is generally the same for each kind of ion implantation. The values of peak volume dopant concentrations and the values of kurtosis increase together with the energy of the implanted ions. On the contrary, the values of range straggling and skewness decrease together with ion energy, The values of the projected range are approximately constant for the ACS case, slightly increase for N^+ ions and slightly decrease for N_2^+ ions.

The change in the value of peak volume dopant concentrations is close to zero for ACS, negative for N^+ ions and positive for N_2^+. The range of the change for all profiles spans from -25% to 32%.

On the contrary, the change in the projected range is positive for ACS and N^+ ions, and negative for N_2^+. In this case, the changes for all data are in the range from about -21% to 41%.

The range straggling is negative for ACS and N_2^+, and mixed for N^+, in the range from about -35% to 18%.

The kurtosis and the skewness show the largest changes in value, especially for ACS and N_2^+ ions. The change in kurtosis is from about -74% to 77%, and the change in skewness is from about -178% to 8% (nearly 190% for all the data).

Table 3. The percentage change of depth profiles data in comparison to the values obtained for $N^+ + N_2^+$ profiles

| Implanted ions		Change of value (%)				
		Peak volume dopant concentration	Projected range	Range straggling	Kurtosis	Skewness
5 kV						
without mass separated beam	$N^+ + N_2^+$	-	-	-	-	-
	ACS	-1.9	1.9	-9.1	-33.9	-38.1
with mass separated beam	N^+	-25.3	34.6	18.2	-30.9	-45.2
	N_2^+	19.6	-17.3	-27.3	-73.6	7.7
50 kV						
without mass separated beam	$N^+ + N_2^+$	-	-	-	-	-
	ACS	-3.9	0.6	-14.3	-33.1	-63.9
with mass separated beam	N^+	-30.4	40.5	15.9	-32.6	-77.1
	N_2^+	17.4	-20.9	-31.2	-28.7	-61.7
500 kV						
without mass separated beam	$N^+ + N_2^+$	-	-	-	-	-
	ACS	17.8	1.3	-22.8	76.7	-173.8
with mass separated beam	N^+	-5.7	41.3	-4.7	7.9	-177.5
	N_2^+	31.8	-21.2	-35.3	44.4	-146
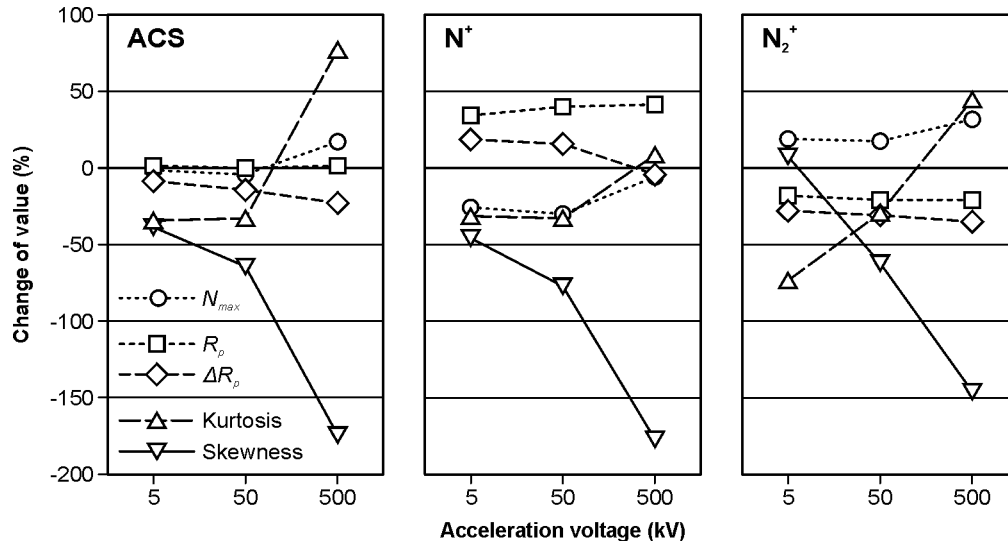
Figure 7. The graphical presentation of changes in the value of peak volume dopant concentrations N_{max}, projected range R_p, range straggling ΔR_p, kurtosis and skewness

Globally, the value of the change in peak volume dopant concentrations, projected range and range straggling is relatively low for ACS for all ion energies (in comparison to the ion implantation of $N^+ + N_2^+$). A larger change of these parameters appears for N_2^+ and for N^+. The peak shape changes in all cases. The largest value of the change is for an ion energy of 500 keV.

CONCLUSION

Based on the comparison of the modelled depth profiles of nitrogen implanted to W-C-Co material, with the use of implanters with or without direct beam, the following conclusions can be formulated:

1. There are no great differences between the ion implantation with $N^+ + N_2^+$ and N_2^+ beam, especially for the acceleration voltage at the level of 5 kV. This situation is only slightly

76

worse for the acceleration voltage at the level of 50 kV, and completely different for 500 kV, where much greater distances and changes in the shape of the profile are observed.

2. The ion implantation with N^+ beam can't be an equivalent of the implantation with $N^+ + N_2^+$ beam in any case.

3. The ACS profile can be a good equivalent of the implantation with $N^+ + N_2^+$ beam for the ion energy range from several to several dozen kilovolts.

REFERENCES

1. BARLAK M., WILKOWSKI J., WERNER Z., 2016: Ion implantation changes of tribological and corrosion resistance properties of materials used in wood industry, *Annals of Warsaw University of Life Science - SGGW, Forestry and Wood Technology* 94, 19-27.

2. BARLAK M., WILKOWSKI J., BORUSZEWSKI P., WERNER Z., PAŁUBICKI B., 2017: Changes of functional properties of materials used in wood industry after ion implantation processes, *Annals of Warsaw University of Life Science - SGGW, Forestry and Wood Technology* 97, 133-139.

3. BARLAK M., WILKOWSKI J., WERNER Z., 2019: Modelling of the ion implantation modification of WC-Co indexable knives for wood machining, *Annals of Warsaw University of Life Science - SGGW, Forestry and Wood Technology* 106, 57-61.

4. BONNY K., DE BAETS P., PEREZ Y., VLEUGELS J., LAUWERS B., 2010: Friction and wear characteristics of WC-Co cemented carbides in dry reciprocating sliding contact, *Wear* 268, 1504-1517.

5. CHOI S.-H., KANG S.-D., KWON Y.S., LIM S.G., CHO K.K., AHN I.-S., 2010: The effect of sintering conditions on the properties of WC-10wt%Co PIM compacts, *Research on Chemical Intermediates* 36, 743-748.

6. KRIVONOSIENKO A.W., NIKOLAEV A.G., LI S., 2001: Технические описание и инструкция по эксплуатаци ионного источника "Титан-3" (Technical descriptions and operating instructions of the ion source "Titan-3"), *Российская Академия Наук - Институт Сильноточной Электроники*, Tomsk, in Russian.

7. MCM, 2014: Monte Carlo method, https://www.sciencedirect.com/topics/engineering/monte-carlo-method

8. MILMAN. YU.V., CHUGUNOVA S., GONCHARUCK V., LUYCKX S., NORTHROP I.T., 1997: Low and high temperature hardness of WC-6 wt%Co alloys. *International Journal of Refractory Metals and Hard Materials* 15, 97-101.

9. OLOVSJÖ S., JOHANSON R., FALSAFI F., BEXELL U., OLSSON M., 2013: Surface failure and wear of cemented carbide rock drill buttons - The importance of sample preparation and optimized microscopy settings, *Wear* 302, 1546-1554.

10. PIRSO J., LETUNOVITŠ S., VILJUS M., 2004: Friction and wear behaviour of cemented carbides, *Wear* 257, 257-265.

11. SHEIKH-AHMAD J.Y., BAILEY J.A., 1999: High-temperature wear of cemented tungsten carbide tools while machining particleboard and fiberboard. *Journal of Wood Science* 45, 445-455.

12. SRIM, 2019: Interactions of ions with matter, http://www.srim.org/

13. SURBHI S., 2017: Differences Between Skewness and Kurtosis, https://keydifferences.com/ differences-between-skewness-and-kurtosis.html

Streszczenie: *Modelowanie procesów implantacji jonów azotu do stosowanych w obróbce materiałów drzewnych wymiennych noży WC-Co, przy użyciu implantatorów bez lub z wiązką bezpośrednią.* W artykule przedstawiono wyniki modelowania głębokościowych profili azotu, implantowanego do materiału W-C-Co, przy użyciu implantatorów bez lub z wiązką bezpośrednią. Modelowanie przeprowadzono przy użyciu metody Monte Carlo, dla jednej wartości dawki implantowanych jonów oraz trzech różnych wartości napięcia przyspieszającego.

Corresponding author:

Marek Barlak
e-mail: marek.barlak@ncbj.gov.pl
National Centre for Nuclear Research Świerk - NCBJ
Plasma/Ion Beam Technology Division (FM2)
7 Andrzeja Sołtana St.
05-400 Otwock, Poland

ORCID ID:
Barlak Marek   0000-0003-1416-7461
Wilkowski Jacek   0000-0001-5798-6761
Werner Zbigniew   0000-0003-1172-0268